

Mangrove Species and Stand Mapping in Gazi Bay (Kenya) using Quickbird Satellite Imagery

G. Neukermans
F. Dahdouh-Guebas
J. G. Kairo
N. Koedam

G. Neukermans

Biocomplexity Research Focus c/o
Laboratory of Plant Biology and Nature
Management
Mangrove Management Group
Vrije Universiteit Brussel - VUB, Pleinlaan 2, B-1050
Brussels Belgium

F. Dahdouh-Guebas

Biocomplexity Research Focus
Département de Biologie des Organismes
Université Libre de Bruxelles, ULB - Campus du
Solbosch, CP 169
Avenue Franklin D. Roosevelt 50, B-1050,
Bruxelles Belgium and
Laboratory of Plant Biology and Nature
Management
Mangrove Management Group
Vrije Universiteit Brussel - VUB, Pleinlaan 2, B-1050
Brussels Belgium and fdahdouh@ulb.ac.be

J. G. Kairo

Kenya Marine and Fisheries Research Institute
PO Box 81651 Mombasa Kenya

N. Koedam

Laboratory of Plant Biology and Nature
Management
Mangrove Management Group
Vrije Universiteit Brussel - VUB, Pleinlaan 2, B-1050
Brussels Belgium

This paper presents an automated method for mangrove stand recognition (delineation and labeling) and species mapping based on fuzzy per-pixel classification techniques of a QuickBird satellite image. The four dominant mangrove species in Gazi Bay (Kenya) are mapped with an overall accuracy of 72 percent, where the two socio-economically most important species are mapped with user accuracies above 85 percent. Mangrove stand maps were compared to visual delineations done by an expert interpreter and the quality was based on the quantity of overlap one has with the other. An overall correspondence up to 86 percent was achieved.

Key Words: Forestry, remote sensing, GIS, vegetation mapping, visual interpretation, delineation accuracy assessment, Point-Centred-Quarter-Method.

INTRODUCTION

Mangroves are intertidal forests of salt-tolerant tree species occurring along tropical and subtropical coasts. Mangroves provide a wide variety of important ecosystem goods and services (e.g. protecting the coast against erosion, wave action and tsunamis, acting as breeding, spawning, hatching and nursing grounds for many marine species, providing subsistence wood and non-wood products to local communities), but their health and persistence are seriously threatened by coastal development projects and various forms of non-renewable exploitation (Farnsworth and Ellison, 1997). The average annual loss rate is estimated at 2.1 percent, losses exceeding those for tropical rain forests and coral reefs (Valiela *et al.*, 2001). Fast declines

continue at assumed rates of 1-20 percent (Alongi, 2002), which will soon lead to a world without mangroves in the absence of appropriate and immediate action (Duke *et al.*, 2007). Therefore, the mangroves that remain are amongst the Earth's most valuable and threatened natural systems and require urgent rational management at the local, regional and global level (UNEP-WCMC, 2006).

Remote sensing (RS) in combination with field survey offers an ideal method to assess the status of mangrove forests and their environment (Green *et al.*, 2000). Mapping mangroves at the species level is required for a thorough understanding of mangrove biodiversity studies and mangrove management (Kairo *et al.*, 2002). Past studies have shown that accurate discrimination of mangrove species is not possible with moderate spatial resolution (>10m) satellite sensors (e.g. Landsat TM, Landsat MSS and SPOT XS) enabling only broad separation of mangroves from surrounding vegetation (e.g. Kay *et al.*, 1991) or differentiation of mangroves into broad classes based on density/age (e.g. Jensen *et al.*, 1991) or on association of species (Dutrieux *et al.*, 1990). Only since very high spatial resolution (VHR) imagery with (sub-) metre resolution became publicly available, mapping mangroves at the species level became feasible with satellite imagery: recent studies have shown that species discrimination is possible with VHR multispectral IKONOS and QuickBird imagery (Wang *et al.*, 2004; Kovacs *et al.*, 2005) and with hyperspectral CASI imagery (Held *et al.*, 2003), although these studies were conducted in mangrove forests dominated by only a few species and less than four mangrove species were mapped.

Both stand delineation and species mapping are cornerstones of forest inventory mapping and key elements to forest management decision making. Most vegetation stand maps made with the help of RS are based on visual interpretation of aerial photographs or VHR satellite imagery. The basic mapping scenario involves delineation and labelling of homogeneous vegetation patches based on the knowledge of the interpreter and augmented with field visits to the area being mapped. Labels are provided concerning the properties of the vegetation within the patch (e.g. dominant species, height and density of the vegetation) inferred from tone, shape, texture, pattern, site, context and association observed

in the imagery (Verheyden *et al.*, 2002). Visual interpretation is both very time-consuming (in part due to digitisation) and suffers from the subjectivity of the interpreter, meaning that the outputs of visual interpretation will be as good or bad as the interpreter, and will vary from interpreter to interpreter (Green *et al.*, 2000). Therefore automation of this process is required. New and improved mapping techniques are constantly being sought in terms of speed, consistency, accuracy, level of detail and overall effectiveness (Leckie *et al.*, 2003). Franklin *et al.* (2001) found that digital first and second order texture measures were useful in distinguishing forest stands of different age classes with panchromatic IKONOS imagery. Leckie *et al.* (2003) achieved semi-automatic stand boundary delineation and species composition estimation of a young conifer stand of simple structure using CASI (Compact Airborne Spectrographic Imager) data with a spatial resolution of 60cm.

This paper investigates the potential of QuickBird satellite imagery and conventional per-pixel techniques for mangrove species mapping and stand recognition (delineation and labelling). It addresses difficulties with the use of the Point-Centred-Quarter-Method (PCQM) for collection of reference data for mangrove species mapping and suggests an improved PCQM protocol.

MATERIALS AND METHODS

Study site

Gazi (Maftaha) Bay (4°25'S and 39°30'E) is a shallow, tropical coastal water system situated in southern Kenya, approximately 47km south of Mombasa. The total area of the Bay, excluding the area covered by mangroves, is about 1000ha. The mangrove forest of Gazi Bay covers about 600ha. All nine East-African mangrove species have been reported in Gazi Bay: *Avicennia marina* (Forssk.) Vierh., *Bruguiera gymnorhiza* (L.) Lam., *Ceriops tagal* (Perr.) C.B. Robinson, *Heritiera littoralis* Dryand., *Lumnitzera racemosa* Willd., *Rhizophora mucronata* Lam., *Sonneratia alba* Sm., *Xylocarpus granatum* Koen and *X. moluccensis* (Lamk.) Roem. (nomenclature according to Tomlinson, 1986). The 10th mangrove species, *Pemphis acidula* Forst., although found in Gazi Bay, has not been included, as it is mostly referred to as an associate species. The mangrove forests of Gazi have been

class	training site field description			CSPMS FCC ^c image description			
	vegetation	canopy cover	soil colour and type	colour	texture	structure	
Avicennia marina	AGazi	landward <i>Avicennia marina</i> closest to Gazi village	50-60%	black sand	orange-pink	rough, irregular	crowns not discernible
	AMD	landward <i>Avicennia marina</i> with medium dense canopy	30-50%	black sand	green-blue	blurry	crowns difficult to separate
	ALD	landward <i>Avicennia marina</i> with low density canopy	20-30%	brown sand	light blue-blue	wrinkled foil	crowns not discernible
	AS	seaward <i>Avicennia marina</i>	60-70%	black sand	yellow-pink	of crown: cauliflower	crowns easily discernible: round, large crowns
	Ashrubs	landward shrubs of <i>Avicennia marina</i>	10-20%	white sand	white-light blue	rough	discontinuous canopy
Ceriops tagal	CGazi	<i>Ceriops tagal</i> closest to Gazi village	70-80%	black mud	green-brown	smooth, woolly, blurred	continuous canopy
	CCM	<i>Ceriops tagal</i> in Central mangrove area	60-70%	black mud	green-blue	smooth	continuous canopy
	CNFP	<i>Ceriops tagal</i> at NFP ^a	80-90%	brown sand	brown-green	woolly, blurred	continuous canopy
	CNMak	<i>Ceriops tagal</i> North of Makongeni river	40-50%	white sand	dark blue	smooth, blurred	continuous canopy
	CWMak	<i>Ceriops tagal</i> West of Makongeni river	40-50%	black mud	green-blue	woolly, blurred	discontinuous canopy
	CMD	<i>Ceriops tagal</i> with medium density canopy	50-60%	black mud	blue	woolly, blurred	continuous canopy
	CLD	<i>Ceriops tagal</i> with low density canopy	20-30%	white sand	light blue	woolly, blurred	continuous canopy
Rhizophora mucronata	REKin	<i>Rhizophora mucronata</i> in East Kinondo region	60-70%	black mud and dead coral	dark green	rough, irregular	discontinuous canopy
	RPlant	<i>Rhizophora mucronata</i> at KMFR ^b plantation	80-90%	black mud	bright red	smooth	continuous canopy
	RWMak	<i>Rhizophora mucronata</i> West of Makongeni river	60-70%	black mud	orange-red	shingle	shingle
	RMiddle	<i>Rhizophora mucronata</i> in the Central Mangrove	80-90%	black mud			
Sonneratia alba	SA	<i>Sonneratia alba</i> South of Central Mangrove	30-40%	black mud	dark blue	rough	crowns not discernible except as individual trees surrounded by water (small to large sized, irregularly shaped crowns)

aNew Fishermen's Place. bKenya Marine and Fisheries Research Institute. cContrast-stretched pansharpened multispectral False Colour Composite

Table 1. Description of image class training sites in the field in terms of vegetation type, percentage canopy cover, top substrate colour and soil type and on the image in terms of colour, texture and structure of the stand on the contrast-stretched pan-sharpened multispectral false colour composite image (CSPMS FCC). The image description of the classes was used as a stand interpretation key for visual interpretation.

exploited for many years e.g. for wood used for industrial fuel (in the chalk, limestone and brick industries in the 1970s) and building poles (Kairo, 1995; Dahdouh-Guebas *et al.*, 2000b).

Field survey

A field mission was conducted in July-August 2003 using the transect PCQM of Cottam and Curtis (1956) as later described by Cintrón and Schaeffer Novelli (1984) and revised by Dahdouh-Guebas and Koedam (2006) for assessment of mangrove forest structural parameters such as density, basal area and frequency. In each sample

point at 10 (or 20m) intervals, four distance-limited quadrants of 5x5m² (or 10x10m²) were established at 90° with respect to the navigational direction. In each quadrant the distance to the closest adult tree was measured with a hand-held laser distometer (Leica Geosystems Disto Lite 4), their species recorded and their G₁₃₀ (the girth at 130cm height along the main tree stem) were measured. The PCQM is a very convenient field method, with a satisfactory to good accuracy (Dahdouh-Guebas and Koedam, 2006) and allowing fairly rapid forestry surveys, which is important in the mangrove tidal ecosystem. The

method was also applied to younger vegetation layers in a larger research framework on vegetation dynamics. GPS locations of begin, middle and end points of transects were recorded with Garmin's GPS III during several minutes, until the GPS position stabilized.

Satellite image pre-processing

A Standard QuickBird satellite panchromatic-multispectral (0.7m-2.8m spatial resolution) bundled image was acquired in October 2002. QuickBird Standard Imagery products are radiometrically corrected, sensor corrected, geometrically corrected (absolute geo-location accuracy of 23m), and mapped to a cartographic projection. The geometric correction was further refined with the QuickBird Rational Polynomial Coefficient model of the first order using 47 easily recognizable and well spread ground control points, recorded with Garmin's GPS III during several minutes, until the GPS position stabilized. The total RMS error was 5.73 metres.

Atmospheric correction was not necessary in this case as atmospheric reflectance is very unlikely to vary much over the study area (4x4km²) and during the acquisition time (< ±1 hour). Pansharpening was done with the principal component resolution merge of ERDAS Imagine 8.7. Mangrove was separated from non-mangrove vegetation manually. Further masking out of pixels corresponding to water and sand led to a contrast stretch, enhancing visual interpretability of the multispectral (pan-sharpened) imagery.

Mangrove species and stand mapping

Training sites were selected visually on the satellite image prior to the field work and then visited in the field. Training sites were selected for the most common species encountered in the mangroves of Gazi Bay: *Avicennia marina* (Amar), *Ceriops tagal* (Ctag), *Rhizophora mucronata* (Rmuc) and *Sonneratia alba* (Salb). The remaining six species did not form large enough mono-specific patches for training site selection and are assumed to

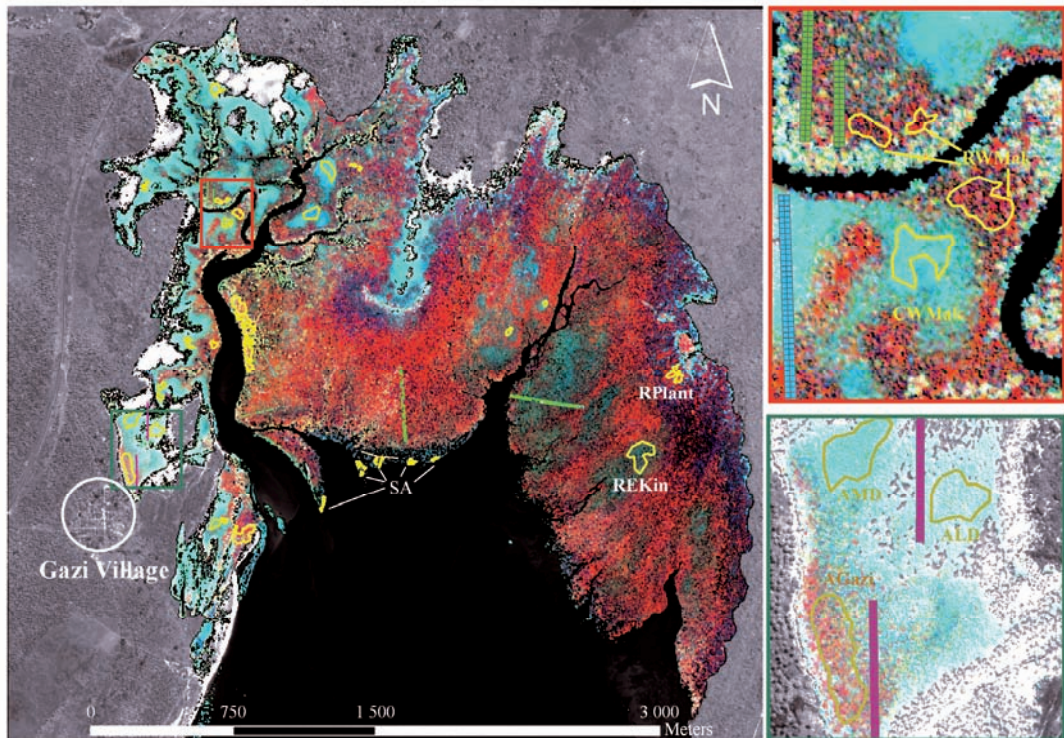


Figure 1. Contrast-stretched pan-sharpened multispectral QuickBird satellite image false colour composite, showing the locations of the PCQM-transects, Gazi Village and the image training sites (in yellow). See Table 1 for abbreviations. Explanation of the colours on the transects: *Avicennia marina* in pink, *Ceriops tagal* in blue, *Rhizophora mucronata* in green, *Sonneratia alba* in white and empty quadrants in orange.

cover less than 10 percent of the forest altogether (*pers. obs.*), but maybe ecologically important. Several spectral manifestations for the same species were found. A description of the image classes' training sites (vegetation type, canopy cover and soil colour and type) in the field and an image description in terms of colour, texture and structure for the contrast-stretched pan-sharpened false colour composite image is given in Table 1. Training sites are shown in Figure 1, together with the location of the PCQM-transects.

Mangrove mapping was realized through fuzzy classification of the contrast-stretched multispectral image. This fuzzy method takes into account the affinity of a pixel and its neighbours to several image classes. The centre pixel is assigned the class with the maximum $T[k]$, the total weighted inverse Mahalanobis distance of all the classes in the neighbourhood window of the centre pixel:

$$T[k] = \sum_{i,j=1}^s \frac{w_{ij}}{D_{ij}[k]} \quad \text{where} \quad D_{ij}[k] = (X_{ij} - m_k)^T C_k^{-1} (X_{ij} - m_k)$$

where i and j are the row and column indices of the pixels in the neighbourhood window of size $s \times s$, w_{ij} is the weight table for window pixel (i,j) , $D_{ij}[k]$ is the Mahalanobis distance between the feature vector of pixel (i,j) (X_{ij}) and the class k mean vector (m_k), T denotes the matrix transpose and C_k is the covariance matrix for class k (ERDAS Field Guide, 2002; Tso and Mather, 2001). Weights w_{ij} decrease linearly with distance from the centre pixel ($w_{ij}=1$) to 0.5 at the edges. A neighbourhood window of size 3×3 pixels was chosen for mangrove species mapping, removing speckle in the classification, smoothing the classification, while preserving enough detail. Mangrove stand mapping was done using a 7×7 pixel neighbourhood window followed by an elimination of continuous groups of pixels (including the diagonal pixels) belonging to the same image class covering less than 500m^2 , replacing the values of pixels in these groups with the value of nearby larger groups.

Visual delineation of mangrove stands was done independently by three interpreters with no experience in image interpretation and no knowledge of mangroves, on print-outs (scale 1:3 000) of the false colour composite of the contrast-stretched pan-sharpened imagery

using slides and pens. A composite delineation, combining the three visually interpreted results (in most cases highly correspondent, in some cases complementary), was digitized on screen by the first author on the same scale in a GIS-environment (ArcGIS version 8.3). Labeling of vegetation stands was also done by the first author, based on field knowledge and a stand interpretation key (Table 1), which included: a description of training site features such as colour, texture, structure and shape of individual tree crowns (when distinguishable).

Accuracy assessment

Transect PCQM data were used for classification accuracy assessment as it was assumed that each sampled adult tree is the dominant species in the quadrant ($5 \times 5\text{m}^2$ or $10 \times 10\text{m}^2$) in which it is recorded and that this layer represented the remotely sensed canopy in the majority of the forest assemblages (e.g. Dahdouh-Guebas *et al.* 2000a). If no adult tree had its stem within a quadrant, that quadrant was classified as *empty*. These field data are overlaid on the species classification, where each pixel can be considered to represent the dominant image class in an $8.4\text{m} \times 8.4\text{m}$ square (3×3 neighbourhood window) (Tso and Mather, 2001). The accuracy was assessed by means of an error matrix, giving overall (OA), user's (UA) and producer's (PA) accuracy and κ (Congalton *et al.*, 1983) and τ (Ma and Redmond, 1995) coefficients. Each record in the error matrix stores the area (in m^2) of each image class within each PCQM species class. Masked pixels (which correspond to water and sand) are considered empty (containing no mangrove) and form class *Empty*. Training sites and PCQM transects did not overlap, ensuring the independence of the reference data for species mapping.

Accuracy assessment of automatically delineated stands is a combination of classification/labelling accuracy and delineation accuracy. Classification accuracy was assessed by means of an error matrix, where the visual interpretation was considered as reference data. These are independent of the classification since visual interpretation is done using an objective stand description (interpretation key in Table 1). Delineation accuracy revolves around the questions of how well the visual delineations

		Classification					Row total	Samples	PA
		<i>Amar</i>	<i>Ctag</i>	<i>Rmuc</i>	<i>Salb</i>	Empty			
Field data	<i>Amar</i>	4892	329	533	8	933	6695	250	0.73
	<i>Ctag</i>	<u>1756</u>	5802	<u>2125</u>	0	212	9895	382	0.59
	<i>Rmuc</i>	<u>3222</u>	337	16621	172	16	20368	415	0.82
	<i>Salb</i>	24	0	149	855	251	1279	50	0.67
	Empty	329	0	102	361	392	1184	48	0.33
Column total		10223	6468	19530	1396	1804	39421	1145	
UA		0.48	0.9	0.85	0.61	0.22			
OA: 0.73		κ: 0.57			τ: 0.62				

Table 2. Error matrix of the mangrove species classification (*Avicennia marina* (*Amar*), *Ceriops tagal* (*Ctag*), *Rhizophora mucronata* (*Rmuc*) and *Sonneratia alba* (*Salb*)), areas given in m², the number of field samples (PCQM-observations) per species is shown in the Samples column. OA: overall accuracy, UA: user accuracy, PA: producer accuracy, underlined numbers: errors due to overtopping of one species by the other.

are matched by automatically delineated stands and how well each automatically delineated stand represents a visual stand, and was done following Leckie *et al.* (2005), who developed a method for accuracy assessment of tree crown recognition. This accuracy depends on the quantity of overlap visual delineations have with automatic delineation and *vice versa*. A total of 16 categories of overlap were defined varying from a perfect to a poor match (see Appendix). About 20 percent of the visual delineations (70 random polygons) and automatic delineations (180 random polygons) were used in the assessment of delineation accuracy.

RESULTS AND DISCUSSION

Field Survey

In total, 15 transects were sampled: 13 transects of 200m length with 5x5m² quadrants and two transects of 400m length with 10x10m² quadrants in the most extensive mangrove stands, totalling 1 145 quadrant species observations. The positional accuracy of the 47 GPS observations at begin, middle and end-points of the transects ranged from 2.0 to 10.3m and averaged 5.32 ± 2.03m.

Mangrove species mapping

All quadrant species observations were digitized in a vector layer (ArcGIS 8.3) and used in the accuracy assessment of the mangrove species map (Table 2). The OA of the mangrove species map was rather low (73 percent), compared to other studies in mangrove remote sensing using

VHR imagery (e.g. Wang *et al.*, 2004). This may be attributable to the lower number of species being mapped in other studies and the fact that it is not clearly mentioned which reference data are being used. Other causes for these low accuracies are: (i) the PCQM species recording does not necessarily correspond to the remotely sensed canopy, due to overtopping of one species by the other, especially in areas of mixed species composition (e.g. adults of the species *Ctag* or *Rmuc* are overtopped by adults of the taller growing *Amar* species, or *Ctag* trees are overtopped by *Rmuc* trees; underlined numbers in Table 2) (ii) inaccurate location of the PCQM quadrants on the image due to (a) the positional inaccuracy of the GPS readings at the beginning, middle and end of each transect, especially under dense canopy and (b) the inaccuracy of the image geometric correction (being 5.73m, which is large compared to the size of a PCQM quadrant, *i.e.* 5 or 10m) (Neukermans, 2004).

Rmuc and *Ctag*, the two socio-economically most important species in this study area (Dahdouh-Guebas *et al.*, 2000b; 2004; Van Tendeloo, 2004), were mapped with UA above 85 percent. The very low PA of the *empty* observations can be attributed to the fact that quadrants where no adult tree was located are not necessarily empty, as they can contain juvenile trees or can be covered by the canopy of trees which do not have their stem in that quadrant. The confusion between *Salb* and *Empty* can be explained by the fact that *Salb*, occurring at the most seaward edge of the

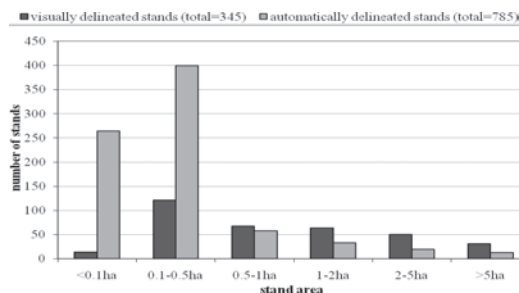


Figure 3. Patch size distribution of visually and automatically delineated stands. Stand areas are given in hectares.

stand map was 64 percent; a classification being 56 percent ($T_s=0.56$) better than one resulting from chance. Classes with an acceptable proportion (>60 percent) of pixels assigned to that class by the classifier that are in agreement with the visual labelling (user's accuracies) are: AS, AGazi, Ashrubs, CMD, CNMak, RMiddle, RWMak, REKin and SA. Classes with an acceptable proportion (>60 percent) of pixels visually assigned to that class that are assigned to the same class by the classifier (producer's accuracies) are: AS, RPlant, RWMak, REKin and SA. Out of a total of 63 large errors 33 errors are errors between classes of the same species. Another 20 errors are errors between *Ctag* and *Amar* classes. Grouped by species, the OA is 86 percent, with all UA and PA above 60 percent and 72 percent more pixels were classified correctly than would be expected by chance alone ($K_s=0.72$). Stands dominated by the species *Rmuc* are most accurately mapped (UA:91%, PA:94%), followed by stands dominated by *Amar* (UA:77%, PA:67%), *Salb* (UA:79%, PA:62%) and *Ctag* (UA:60%, PA:65%). This shows that the automatically delineated stands are much more accurate in discriminating between stands with different dominant mangrove species, than in discriminating between stands with the same dominant species, but with different canopy cover.

Delineation accuracy. (a) *How well are visual delineations recognized by automatically delineated stands?* About one fifth (17 percent) of the visual delineated stands are perfectly to well matched by automatic delineations (categories 1 and 2, see Appendix) and 24 percent of the visual delineations were absorbed in a much bigger automatic delineation (category 4). This was especially the case with

polygons labelled RWMak: there are two large (198ha and 46ha) *Rmuc* dominated (RWMak) automatic delineations, which are a perfect split of 56 RWMak visual delineations. The visual delineations represent stands dominated by *Rmuc*, interspaced with different species, which makes them visually different, but through fuzzy and elimination filtering, information on the other species is lost, resulting in one large *Rmuc* automatic delineation. Another 24 percent of the visual delineations were perfectly to well split into several automatic delineations (categories 5, 6 and 7), which can still be considered good matches, because the visual delineation is represented by a group of automatic delineations, mostly belonging to the same species. This is because the visual interpreter exploits spatial context and neighbourhood and therefore tends to connect neighbouring similar stands into one bigger visual delineation. The remaining 34 percent of the visual delineations have poor matches with automatic delineations (categories 3, 8 and 16). A possible source of error might be the spectral overlap between the image classes.

(b) *How well do automatically delineated stands represent visually delineated stands?* Few automatic delineations (11 percent) had perfect to good visual counterparts (categories 1 and 9). More than half (60 percent) of the automatic delineations were absorbed in larger visual delineations (category 11). This is a consequence of the much larger number and much smaller sizes of automatic delineations compared to visual delineations. These errors are possibly caused by (i) the fact that each pixel in the image represents 2^{44} (4 bands at 11-bit resolution) unique spectral signatures and the incapability of the human eye to distinguish that many levels of tones and hues in an image, (ii) quality loss due to printing and display on a computer screen at a large scale and (iii) visual misinterpretation. Moreover, the false colour composite is displayed on the screen by projecting the near-infrared band through the red, the green band through the green and the blue band through the blue colour guns of the monitor. Thus the information from the red band (which is available in digital image classification) cannot be used in visual interpretation. Visual interpretation therefore does not come close to utilizing the full information content of an image (Green

Automatically delineated stands (classification)

Species	Ctag										Rmuc				SA	Row total	PA _c	PA _s				
	Amar					Ctag					RMiddle	RPlant	RWMak	REKin	SA							
<i>Amar</i>	AS	AGazi	AMD	ALD	Ashrubs	CNFP	CGazi	CCM	CMD	CWMak	CNMak	CLD	RMiddle	RPlant	RWMak	REKin	SA	60.83	0.62			
	AS	37.44	0.29	1.17	1.31	0.07	0.35	0.18	0.03	0.01	0.31	0.00	0.54	0.30	0.04	18.97	0.12	0.70	11.63	0.27		
	AGazi	2.38	3.19	<i>1.32</i>	2.77	0.29	0.12	0.04	0.00	0.00	0.00	0.41	0.00	0.01	1.11	0.00	0.00	0.00	9.25	0.27		
	AMD	1.00	0.65	2.53	1.75	0.61	0.61	0.07	0.02	0.00	<i>0.09</i>	0.00	0.99	0.00	0.03	0.93	0.00	0.00	14.14	0.38		
	ALD	0.57	0.04	<i>0.69</i>	5.40	2.85	0.14	0.01	0.00	0.00	0.00	3.35	0.00	0.00	1.09	0.00	0.00	0.00	21.38	0.47	0.67	
	Ashrubs	0.09	0.05	0.20	3.40	10.00	0.39	0.07	0.00	0.02	0.38	0.00	6.77	0.00	0.00	0.00	0.00	0.00	8.20	0.28		
<i>Ctag</i>	CNFP	0.21	0.00	0.30	0.48	0.23	2.28	<i>0.20</i>	1.32	0.30	1.55	0.02	1.10	0.00	0.00	0.08	0.08	0.04	2.55	0.09		
	CGazi	0.29	0.14	0.24	0.07	0.01	0.96	0.24	0.00	0.00	0.02	0.00	0.02	0.00	0.00	0.55	0.00	0.00	16.69	0.33		
	CCM	1.11	0.00	0.14	0.09	0.00	1.17	0.00	5.54	0.00	0.06	0.00	0.11	0.10	0.00	7.71	0.62	0.04	7.54	0.33		
	CMD	0.05	0.01	0.41	0.15	0.05	0.55	0.00	0.94	2.48	0.94	0.11	1.51	0.00	0.00	0.34	0.00	0.00	2.79	0.14		
	CWMak	0.29	0.00	0.26	0.00	0.09	0.85	0.01	0.18	0.00	0.38	0.00	0.19	0.00	0.00	0.53	0.00	0.00	5.46	0.18		
	CNMak	0.32	0.03	0.36	0.00	0.00	0.05	0.00	2.00	0.18	0.70	0.97	0.78	0.00	0.00	0.08	0.00	0.00	8.43	0.56	0.65	
	CLD	0.10	0.00	0.35	0.49	1.51	0.11	0.02	0.16	0.28	0.56	0.00	4.76	0.00	0.00	0.06	0.03	0.00	71.86	0.41		
<i>Rmuc</i>	RMiddle	0.64	0.00	0.00	0.00	0.00	0.00	0.07	0.00	0.00	0.00	0.00	0.49	29.32	17.49	22.74	1.07	0.04	22.62	0.62		
	RPlant	0.30	0.00	0.00	0.04	0.00	0.00	0.01	0.00	0.00	0.00	0.64	0.24	14.03	7.15	0.21	0.00	0.00	256.74	0.81		
	RWMak	12.23	0.37	0.22	0.07	0.01	1.42	0.08	2.12	0.08	0.34	0.00	0.68	3.20	13.94	207.09	14.06	0.84	47.10	0.72	0.94	
	REKin	0.55	0.00	0.00	0.00	0.00	0.16	0.00	0.72	0.00	0.16	0.00	0.00	0.19	0.01	11.09	33.84	0.38	12.66	0.62	0.62	
<i>Salb</i>	SA	1.06	0.00	0.00	0.04	0.03	0.33	0.00	0.00	0.00	0.38	0.00	0.00	2.01	0.00	0.88	0.04	7.87	50.09	9.91		
total		58.63	4.76	7.20	16.06	15.77	9.48	0.92	13.10	3.36	5.86	1.09	22.34	35.36	45.55	280.40	50.09	9.91				
UA _c		0.64	0.67	0.35	0.34	0.63	0.24	0.26	0.42	0.74	0.07	0.88	0.21	0.83	0.31	0.74	0.68	0.79				
UA _s					0.77							0.60					0.91	0.79				

Column	OA _c	OA _s
	0.64	0.86
	0.52	0.69
	0.56	0.72

Table 3. Error matrix of the mangrove stand classification, entries in hectares. The c-subscript in UA (user accuracy), PA (producer accuracy), OA (overall accuracy), K and T refers to the accuracy measures per image class, the s-subscript refers to the accuracy measures when image classes are grouped per mangrove species; numbers in bold: row elements larger than 20 percent of the diagonal element, numbers in italic: column elements larger than 20 percent of the diagonal element.

et al., 2000). Only 2 percent of the automatic delineations were split into several visual stands (categories 12, 13 and 14). The remaining 28 percent of the automatic delineations were categorized as poorly matched by a visual delineation (categories 10, 15 and 16).

CONCLUSIONS

We conclude that it is possible to accurately (OA: 73 percent) map the four dominant mangrove species in Gazi Bay through per-pixel classification of multispectral QuickBird satellite imagery. However, great care should be taken in the collection of ground reference data to determine classification accuracy. The Point-Centred-Quarter-Method, used for determining forest structural attributes, can be upgraded for collection of ground reference data in classification accuracy assessment through the addition of a canopy layer that describes the remotely sensed canopy in terms of percentage total cover and percentage cover per species, rather than using the species recordings of adult trees for this purpose (e.g. by Dahdouh-Guebas et al., 2000a). Other shortcomings of the PCQM for assessment of forest structural attributes are also dealt with by Dahdouh-Guebas and Koedam (2006).

Automatic delineation and labelling of mangrove stands based on dominant species and total cover was compared to visual delineations done by an expert interpreter. An overall correspondence of 64 percent was obtained for automatically delineated stand labelling. When only dominant species were taken into account, the OA of automatic stand labelling increased to 86 percent. The total number and the patch size distribution of automatically delineated and visually delineated stands differed greatly. Generally more patches of smaller size were automatically recognized. Only 11-17 percent of the automatically and visually delineated stands were perfectly to well matched. Improvements can be expected if the minimum size of automatically delineated assemblages is increased or by grouping classes together.

Further research is needed to determine the applicability of these fuzzy techniques for mangrove species and assemblage mapping in other mangrove forests.

REFERENCES

- Alongi, D.M. (2002) Present state and future of the world's mangrove forests. *Environmental Conservation*, vol. 29, no. 3, pp. 331-349.
- Cintrón, G. and Schaeffer Novelli, Y. (1984) Methods for studying mangrove structure. In : *The mangrove ecosystem : research methods*. Snedaker, S.C. and J.G. Snedaker, eds. UNESCO, Paris, France, pp. 91-113.
- Congalton, R.G., Oderwald, R. and Meade, R. (1983) Landsat classification accuracy using discrete multivariate analysis statistical techniques. *Photogrammetric Engineering and Remote Sensing*, vol. 49, pp. 1671-1678.
- Cottam, G. and Curtis, J.T. (1956) The use of distance measures in phytosociological sampling. *Ecology*, vol. 37, no. 3, pp. 451-460.
- Dahdouh-Guebas, F., Verheyden, A., De Genst, W., Hettiarachchi, S. and Koedam, N. (2000a) Four decade vegetation dynamics in Sri Lankan mangroves as detected from sequential aerial photography : a case study in Galle. *Bulletin of Marine Science*, vol. 67, pp. 741-759.
- Dahdouh-Guebas, F., C. Mathenge, J.G. Kairo & N. Koedam (2000b) Utilization of mangrove wood products around Mida Creek (Kenya) amongst subsistence and commercial users. *Economic Botany*, vol. 54, no. 4, pp. 513-527.
- Dahdouh-Guebas, F., Van Pottelbergh, I., Kairo, J.G., Cannicci, S., and Koedam, N. (2004) Human-impacted mangroves in Gazi (Kenya): predicting future vegetation based on retrospective remote sensing, social surveys, and distribution of trees. *Marine Ecology Progress Series*, vol. 272, pp. 77-92.
- Dahdouh-Guebas, F. and Koedam, N. (2006) Empirical estimate of the reliability of the use of the Point-Centred Quarter Method (PCQM): solutions to ambiguous field situations and description of the PCQM+ protocol. *Forest Ecology and Management*, vol. 228, pp. 1-18.
- Duke, N.C., Meynecke, J.-O., Dittmann, S., Ellison, A.M., Anger, K., Berger, U., Cannicci, S., Diele, K., Ewel, K.C., Field, C.D., Koedam, N., Lee, S.Y., Marchand, C., Nordhaus, I., Dahdouh-Guebas, F. (2007) A world without mangroves? *Science*, vol. 317, pp. 41-42.

- Dutrieux, E., Dennis J., and Populus, J. (1990) Application of SPOT data to a base-line ecological study of the Lahakam Delta mangroves, East Kalimantan, Indonesia. *Oceanologica Acta*, vol. 13, pp. 317-326.
- ERDAS Field Guide (2002) ERDAS Field Guide, Leica Geosystems, GIS & Mapping Division, Atlanta, Georgia, USA. Sixth Edition.
- Farnsworth, E.J. and Ellison, A.M. (1997) The global conservation status of mangroves. *Ambio*, vol. 26, no. 6, pp. 328-334.
- Franklin, S.E., Wulder, M.A., and Gerylo, G.R. (2001) Texture analysis of IKONOS panchromatic data for Douglas-fir forest age class separability in British Columbia. *International Journal of Remote Sensing*, vol. 22, pp. 2627-2632.
- Green, E.P., Mumby, P.J., Edwards, A.J. and Clark, C.D. (2000) *Remote sensing handbook for tropical coastal management*. Coastal Management Sourcebooks 3, UNESCO, Paris. x + 316 pp.
- Held, A., Ticehurst, C., Lymburner, L. and Williams, N. (2003) High resolution mapping of tropical mangrove ecosystems using hyperspectral and radar remote sensing. *International Journal of Remote Sensing*, vol. 24, no. 13, pp. 2739-2759.
- Jensen, J.R., Ramset, E., Davis, B.A. and Thoenke, C.W. (1991) The measurement of mangrove characteristics in south-west Florida using SPOT multispectral data. *Geocarto International*, vol. 2, pp. 13-21.
- Kairo, J.G. (1995) Artificial regeneration and sustainable yield management of mangrove forests in Gazi Bay, Kenya. M.Sc. Thesis Botany, University of Nairobi, Nairobi, Kenya: p116.
- Kairo, J.G., Kivyatu, B., and Koedam, N. (2002) Application of remote sensing and GIS in the management of mangrove forests within and adjacent to Kiunga Marine Protected Area, Lamu, Kenya. *Environment, Development and Sustainability*, vol. 4, no. 2, pp. 153-166.
- Kay, R.J., Hick, P.T., and Houghton, H.J. (1991) Remote sensing of Kimberley rainforests. In : *Kimberley Rainforests*, edited by N.I. McKenzie, R.B. Johnston & P.G. Kendrick. Surrey Beatty & sons: Chipping Norton, pp. 41-51.
- Kovacs, J.M., Wang, J. and Flores-Verdugo, F. (2005) Mapping mangrove leaf area index at the species level using IKONOS and LAI-2000 sensors for the Agua Brava Lagoon, Mexican Pacific. *Estuarine, Coastal and Shelf Science* 62: 377–384.
- Leckie, D.G., Gougeon, F.A., Walsworth, N. and Paradine, D. (2003) Stand delineation and composition estimation using semi-automated individual tree crown analysis. *Remote Sensing of the Environment*, vol. 85, pp. 355-369.
- Leckie, D.G., Gougeon, F.A., Tinis, S., Nelson, T., Burnett, C .N. and Paradine, D. (2005) Automated tree recognition in old growth conifer stands with high resolution digital imagery. *Remote Sensing of the Environment*, vol. 94, pp. 311-326.
- Ma, Z. and Redmond, R.L. (1995) Tau coefficients for accuracy assessment of classification of remote sensing data. *Photogrammetric Engineering and Remote Sensing*, vol. 61, pp. 435-439.
- Neukermans, G. (2004) *Remote sensing mangroves in Gazi Bay (Kenya) with very high resolution QuickBird satellite imagery : automated methods for species and assemblage identification*. MSc. Ecological Marine Management thesis, Vrije Universiteit Brussel, Brussels, Belgium.
- Tomlinson, C.B. (1986) *The Botany of Mangroves*. Cambridge Tropical Biology Series, Cambridge University Press, Cambridge, New York, U.S.A.
- Tso, B. and Mather, P.M. (2001) *Classification methods of remotely sensed data*. Taylor and Francis , London, England and New-York, USA
- UNEP-WCMC (2006) *In the front line: shoreline protection and other ecosystem services from mangroves and coral reefs*. UNEP-WCMC, Cambridge, UK 33 pp
- Valiela, I., Bowen, J.L. and York, J.K. (2001) Mangrove forests: One of the world's threatened major tropical environments. *Bioscience*, vol. 51, no. 10, pp. 807-815
- Van Tendeloo, A. (2004) *Veranderingen in traditionele en commerciële mens-ecosysteemrelaties in de mangrovebaai van Gazi (Kenya): etnobiologie, percepties van de lokale gemeenschap en eco-toeristische*

activiteiten. Lic./MSc. Biology thesis, Vrije Universiteit Brussel, Brussels, Belgium.

Verheyden, A., Dahdouh-Guebas, F., Thomaes, K., De Genst, W., Hettiarachchi, S. and Koedam, N. (2002) High resolution vegetation data for mangrove research as obtained from aerial photography. *Environment, Development and Sustainability*, vol. 4, no. 2, pp. 113-133.

Wang, L., Sousa, W.P. and Gong, P. (2004) Integration of object-based and pixel-based classification for mapping mangroves with IKONOS imagery. *International Journal of Remote Sensing*, vol. 25, no. 24, pp. 5655-5668.

ACKNOWLEDGEMENTS

We thank the people from the Kenya Marine and Fisheries Research Institute (KMFRI) for providing logistic support. Much gratitude is due to all people of Gazi, in particular Latifa Salim and family S. Ba'alawy for hosting us, Helen Defever, Anneleen Van Tendeloo, Abubakar Said Hamisi, Imara and Paul Thomas Obade for their practical help in the field. The research was supported by the EC funded project PUMPSEA (FP6 - INCO contract no. 510863), the Flemish Inter-University Council (VLIR) and the Fund for Scientific Research (FWO - Vlaanderen). Kairo's participation in this work was covered by MASMA Programme supported by Western Indian Ocean Marine Science Association (WIOMSA).

APPENDIX

Categories of overlap between visual delineated stands (videls) and automatic delineations (audels) (adapted from Leckie *et al.* 2005). An audel and a videl are considered associated when >10 percent of the audel is covered by the videl and vice versa.

(a) *Videl-centric and audel-centric perfect match*: **1** Perfect match: >75% of a single audel is occupied by a single videl and the audel occupies >75% of the videl.

(b) *Videl-centric (how well the visual stands match with the automatically delineated ones)*: **2** Good match (audel too big): >75% of the videl is occupied by a single audel and only 50-75% of that audel is occupied by the videl. **3** Poor match (audel much too big): >75% of the videl is occupied by a single audel and only

25-50% of that audel is occupied by the videl. **4** Absorption: >75% of the videl is occupied by a single audel and <25% of the audel is occupied by the videl. **5** Videl-centric perfect split (one dominant): A videl that contains a group of audels within it, >75% of each audel's area is occupied by the videl and one of the audels covers >50% of the videl's area **6** Videl-centric perfect split (none dominant): A videl that contains a group of audels within it, >75% of each audel's area is occupied by the videl and none cover >50% of the videl's area **7** Videl-centric good split : A videl that contains a group of audels within it (i.e. 75% of at least one audel is occupied by the videl); at least one audel has only 25-50% of its area occupied by the videl; **8** Videl-centric poor split : A videl that contains a group of audels within it (i.e. 75% of at least one audel is occupied by the videl); at least one audel has <25% of its area occupied by the videl

(c) *Audel-centric (how well automatically delineated stands represent visual stands)*: **9** Good match (audel too small): >75% of the audel is occupied by a single videl and only 50-75% of that videl is occupied by the audel. **10** Poor match (audel much too small): >75% of the audel is occupied by a single videl and only 25-50% of that videl is occupied by the audel. **11** Absorption: >75% of the audel is occupied by a single videl and <25% of the videl is occupied by the audel. **12** Audel-centric perfect split (one dominant): An audel that contains a group of videls within it, >75% of each videl's area is occupied by the audel and one videl covers >50% of the audel's area **13** Audel-centric perfect split (none dominant): An audel that contains a group of videls within it, >75% of each videl's area is occupied by the audel and none cover >50% of the videl's area **14** Audel-centric good split : An audel that contains a group of videls within it (i.e. 75% of at least one videl is occupied by the audel); at least one videl has only 25-50% of its area occupied by the audel; **15** Audel-centric poor split : An audel that contains a group of videls within it (i.e. 75% of at least one videl is occupied by the audel); at least one videl has <25% of its area occupied by the audel

(d) *Other matches*: **16** Poor matches: All other cases of overlapping audels and videls